

Roscovitine Targets, Protein Kinases and Pyridoxal Kinase*[§]

Received for publication, January 21, 2005, and in revised form, June 21, 2005
Published, JBC Papers in Press, June 23, 2005, DOI 10.1074/jbc.M500806200

Stéphane Bach,^a Marie Knockaert,^a Jens Reinhardt,^a Olivier Lozach,^a Sophie Schmitt,^a Blandine Baratte,^a Marcel Koken,^a Stephen P. Coburn,^b Lin Tang,^c Tao Jiang,^c Dong-cai Liang,^c Hervé Galons,^d Jean-Francois Dierick,^e Lorenzo A. Pinna,^f Flavio Meggio,^f Frank Totzke,^g Christoph Schächtele,^g Andrea S. Lerman,^h Amancio Carnero,^h Yongqin Wan,ⁱ Nathanael Gray,ⁱ and Laurent Meijer^{a,j}

From the ^aCNRS, Cell Cycle Group, UPS 2682 & UMR 2775, Station Biologique, BP 74, 29682 Roscoff cedex, Bretagne, France, the ^bDepartment of Chemistry, Indiana University-Purdue University, Fort Wayne, Indiana 46805-1499, the ^cNational Laboratory of Biomacromolecules, Institute of Biophysics, Chinese Academy of Sciences, 15 Datun Road, Chaoyang District, Beijing 100101, China, the ^dLaboratoire de Chimie Organique 2, Université René Descartes, 4 avenue de l'Observatoire, 75270 Paris cedex 06, France, the ^eProteomics Unit, BioVallée, Rue Adrienne Bolland, 6041 Gosseries, Belgium, the ^fDipartimento di Chimica Biologica, Università di Padova, 35121 Padova, Italy, the ^gProQinase GmbH, Breisacher Strasse 117, 79106 Freiburg, Germany, the ^hCentro Nacional de Investigaciones Oncológicas (CNIO), Programa de Terapias Experimentales, c/Melchor Fernandez Almagro No. 3, 28029 Madrid, Spain, and the ⁱGenomics Institute of the Novartis Research Foundation, Department of Chemistry, San Diego, California 92121

(R)-Roscovitine (CYC202) is often referred to as a “selective inhibitor of cyclin-dependent kinases.” Besides its use as a biological tool in cell cycle, neuronal functions, and apoptosis studies, it is currently evaluated as a potential drug to treat cancers, neurodegenerative diseases, viral infections, and glomerulonephritis. We have investigated the selectivity of (R)-roscovitine using three different methods: 1) testing on a wide panel of purified kinases that, along with previously published data, now reaches 151 kinases; 2) identifying roscovitine-binding proteins from various tissue and cell types following their affinity chromatography purification on immobilized roscovitine; 3) investigating the effects of roscovitine on cells deprived of one of its targets, CDK2. Altogether, the results show that (R)-roscovitine is rather selective for CDKs, in fact most kinases are not affected. However, it binds an unexpected, non-protein kinase target, pyridoxal kinase, the enzyme responsible for phosphorylation and activation of vitamin B₆. These results could help in interpreting the cellular actions of (R)-roscovitine but also in guiding the synthesis of more selective roscovitine analogs.

Frequent alteration of protein phosphorylation in human disease is the reason for an exponentially growing investment in the optimization and therapeutic evaluation of small molecular weight, pharmacological inhibitors of protein kinases, the enzymes responsible for protein phosphorylation (reviews in Refs. 1 and 2). Currently 55 kinase inhibitors are undergoing clinical evaluation against diseases such as cancers, inflammation, diabetes, and neurodegeneration. Some, like Gleevec or

Fasudil, have actually achieved a real market success. Nevertheless, the exact mechanism of action and the real range of targets of most of these inhibitors remain largely unknown. Selectivity is usually addressed by testing the inhibitors on a small panel of purified kinases (3, 4), yet this approach is far from covering the estimated 518+ kinases of our genome, nor is it even considering alternative, non-kinase targets. Other ways to tackle the selectivity problem have recently been developed (reviewed in Ref. 5), such as affinity chromatography on immobilized inhibitor (6–13) (reviewed in Refs. 14 and 15), cDNA phage display technology (16), yeast three-hybrid system (17), *in vitro* competition assays (18), or chemical genomics (19).

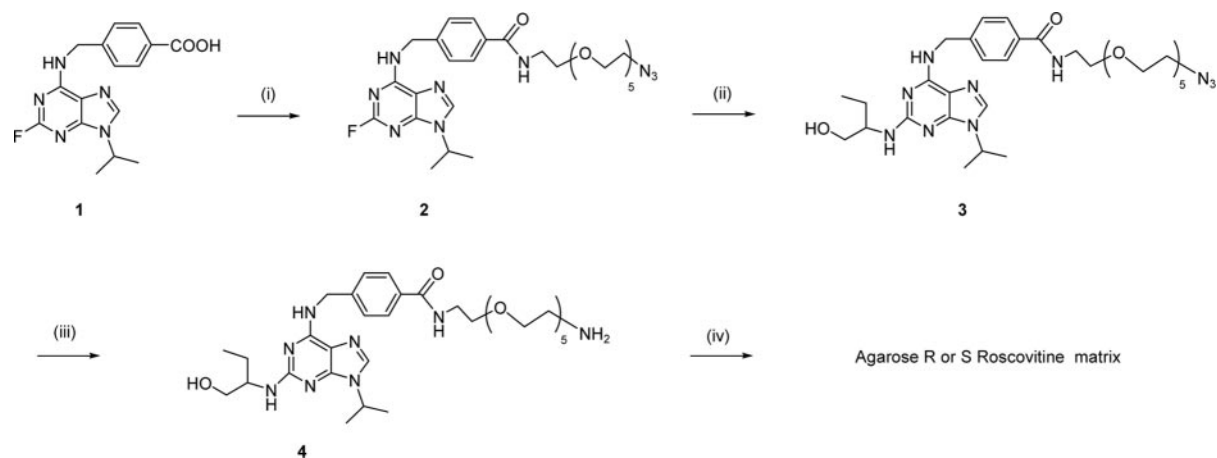
The involvement of cyclin-dependent kinases (CDK)¹ in cell cycle control (20), neuronal cell physiology (21), apoptosis (22), and transcription (23) has inspired considerable interest in this family of kinases. Abnormalities in CDK activity and regulation in cancers (24, 25), viral infections (26), and neurodegenerative disorders, such as Alzheimer (27), Parkinson (28, 29), and Nieman-Pick (30) diseases, and ischemia (31) have encouraged an intensive search for potent and selective pharmacological inhibitors of these kinases (reviewed in Ref. 32). Over 80 small molecular weight inhibitors have been characterized, most of which appear to act by direct competition with ATP for binding to the catalytic cleft. Over 30 of these compounds have been co-crystallized with CDK2 (33) and/or CDK5 (34), confirming their binding in the ATP binding pocket of CDKs. The family of 2,6,9-trisubstituted purines encompasses some of the first CDK inhibitors to be described (reviewed in Refs. 35 and 36). This includes olomoucine (37), roscovitine (38–40) (reviewed in Ref. 36), and purvalanol (41, 42). The (R)-stereoisomer of roscovitine is one of the most frequently studied and used CDK inhibitors. Also referred to as CYC202 or Seliciclib (Cyclacel Ltd., Dundee, UK), (R)-roscovitine is currently being tested in animals (43–47) and humans (48). It has reached the stage of phase 2 clinical trials against lung and breast cancer, and phase 1 trials against glomerulonephritis (49).

* This work was supported by the Ministère de la Recherche/INSERM/CNRS “Molécules et Cibles Thérapeutiques” Program (to L. M.), EEC Grant FP6-2002-Life Sciences & Health, the PRO-KINASE Research Project (to L. M.), Canceropole Grand-Ouest (to L. M.), and Chinese Academy of Sciences Grants (KSCX1-SW-17 and KJCX2-SW-N06) (to T. J. and D. L.). The costs of publication of this article were defrayed in part by the payment of page charges. This article must therefore be hereby marked “advertisement” in accordance with 18 U.S.C. Section 1734 solely to indicate this fact.

[§] The on-line version of this article (available at <http://www.jbc.org>) contains additional text and Tables S1 and S2.

^j To whom correspondence should be addressed. Tel.: 33-0-2-98-29-23-39; Fax: 33-0-2-98-29-23-42; E-mail: meijer@sb-roscoff.fr.

¹ The abbreviations used are: CDK, cyclin-dependent kinase; Me₂SO, dimethyl sulfoxide; MEF, mouse embryonic fibroblasts; PBS, phosphate-buffered saline; PDXK, pyridoxal kinase; Mops, 4-morpholinepropanesulfonic acid; MALDI-TOF, matrix-assisted laser desorption ionization time-of-flight; CK1, casein kinase 1.



SCHEME 1. Preparation of (*R*)- and (*S*)-roscovitine resins. Conditions: (i) 2.0 eq of *N*-ethyldiisopropylamine, 2.0 eq of 2-[2-(2-[2-(2-azido-ethoxy)-ethoxy]-ethoxy)-ethoxy]-ethylamine, 1.0 eq of *O*-(7-azabenzotriazol-1-yl)-*N,N,N',N'*-tetramethyluronium hexafluorophosphate, dimethylformamide, 3 h; (ii) 10 eq of *N*-ethyldiisopropylamine, 40 eq of (*R*)- or (*S*)-(+)-2-amino-1-butanol, *n*-butanol, microwave irradiation, 190 °C, 30 min; (iii) 10% Pd/C, MeOH, H₂, 12 h; (iv) 3 mM linker-bearing (*R*)- or (*S*)-roscovitine (5 ml), Affi-Gel® 10 Gel (Bio-Rad) (5 ml bed volume), triethylamine (10 μl), Me₂SO, 1 h.

Considerable data has accumulated with respect to the effects of roscovitine on a large diversity of cellular models and physiological settings including cell proliferation, virus replication, neurotransmitter release and action, excretion, and apoptosis. (*R*)-Roscovitine is indeed often presented and used as a “selective inhibitor of CDKs.” According to selectivity studies performed on two panels of purified kinases (4, 39), (*R*)-roscovitine indeed appears to be relatively selective for CDKs. However, the existence of a few kinases inhibited at high micromolar concentrations (DYRK1A, ERK1/ERK2, and CK1), and the presence of over 2000 ATP utilizing enzymes (including 518+ kinases) and numerous other nucleotide-binding proteins in the human proteome, suggests that further investigation of the selectivity of (*R*)-roscovitine might be of interest for a better understanding of its cellular and physiological actions.

We here report on the results of our investigation on the targets of (*R*)-roscovitine. We have approached the selectivity problem using three different methods: (i) testing (*R*)-roscovitine on a wide panel of purified kinases and compiling all available data; (ii) identifying roscovitine-binding proteins from various tissues and cells following affinity chromatography purification on immobilized roscovitine; and (iii) investigating the effects of roscovitine on cells deprived of a major target, CDK2. Altogether, the results show that (*R*)-roscovitine is rather selective for CDKs but that it interacts with an unexpected, non-protein kinase target, pyridoxal kinase (PDXK), the enzyme responsible for the phosphorylation and activation of vitamin B₆. These results could be useful to improve the selectivity of roscovitine, but also to interpret its cellular actions in a more detailed manner.

EXPERIMENTAL PROCEDURES

Preparation of (*R*)- and (*S*)-Roscovitine Resins

Azide 2—To a solution of 4-[(2-fluoro-9-isopropyl-9*H*-purin-6-ylamino)methyl]benzoic acid (**1**) (0.22 g, 0.5 mmol) in dimethylformamide (4 ml) was added *N*-ethyldiisopropylamine (0.18 ml, 1.0 mmol), 2-[2-(2-[2-(2-azido-ethoxy)-ethoxy]-ethoxy)-ethoxy]-ethylamine (0.30 g, 1.0 mmol), and *O*-(7-azabenzotriazol-1-yl)-*N,N,N',N'*-tetramethyluronium hexafluorophosphate (0.19 g, 0.5 mmol). The reaction mixture was stirred at room temperature for 3 h and concentrated in vacuum. To the residue was added HCl (1 N, 50 ml) and the mixture was extracted by ethyl acetate (3 × 30 ml). Ethyl acetate layers were combined and washed with brine (30 ml). The drying agent was removed, and the solvent was removed in vacuum. The resulting residue was purified by high performance liquid chromatography (C₁₈ column, eluted with CH₃CN/H₂O with 0.035% trifluoroacetic acid) to afford azide (**2**) as a

colorless oil (0.29 g, 76%). The spectra used was ¹H NMR (methanol-*d*₄), δ 1.59 (d, 6H, *J* = 7.2 Hz), 3.33 (t, 2H, *J* = 4.8 Hz), 3.56–3.68 (m, 24H), 4.75 (septet, 1H), 4.80–4.84 (m, 2H), 7.49 (d, 2H, *J* = 8.0 Hz), 7.81 (d, 2H, *J* = 8.0 Hz), 8.29 (s, 1H); *m/z* [M⁺ + 1] 618.2.

(*S*)-Roscovitine-linker Azide (**3a**)

A solution of azide (**2**) (55 mg, 0.075 mmol), *N*-ethyldiisopropylamine (130 μl, 0.75 mmol), and (*S*)-(+)-2-amino-1-butanol (0.27 g, 3 mmol) in *n*-BuOH (1 ml) in a Smith Process vial was sealed and heated at 190 °C for 30 min using microwave irradiation. The reaction mixture was then concentrated, and water (10 ml) was added. It was extracted with ethyl acetate (3 × 10 ml). The organic layers were combined, washed with brine (10 ml), and dried with Na₂SO₄. The drying agent was removed, and the solvent was evaporated. The resulting residue was purified by high performance liquid chromatography (C₁₈ column, eluted with CH₃CN/H₂O with 0.035% trifluoroacetic acid) to afford the title compound as colorless oil (36 mg, 53%). The spectra used was ¹H NMR (methanol-*d*₄), δ 0.92–1.04 (m, 3H), 1.52–1.58 (m, 1H), 1.59 (d, 6H, *J* = 6.4 Hz), 1.68–1.80 (m, 1H), 3.34 (t, 2H, *J* = 5.2 Hz), 3.56–3.72 (m, 27H), 3.96–4.04 (m, 1H), 4.64–4.72 (m, 2H), 7.49 (d, 2H, *J* = 8.0 Hz), 7.83 (d, 2H, *J* = 8.0 Hz), 8.11 (s, 1H); *m/z* [M⁺ + 1] 687.1.

(*R*)-Roscovitine-linker Azide (**3b**)

(*R*)-Roscovitine-linker azide (**3b**) was synthesized with the same method as described for **3a** using (*R*)-(+)-2-amino-1-butanol (Scheme 1).

(*S*)-Roscovitine-linker Amine (**4a**)

Pd/C (10%, 50 mg) was added to a methanol solution of (*S*)-roscovitine-linker azide (**3a**) (30 mg, 0.045 mmol). It was stirred overnight at room temperature under hydrogen atmosphere and the catalyst was removed by filtration. Methanol was removed in vacuum to afford a colorless oil. It was further purified by high performance liquid chromatography (C₁₈ column, eluted with CH₃CN/H₂O with 0.035% trifluoroacetic acid) to afford the title compound as colorless oil (23 mg, 80%). The spectra used was ¹H NMR (Me₂SO-*d*₆), δ 0.78–0.92 (m, 3H), 1.48 (d, 3H, *J* = 2.8 Hz), 1.50 (d, 3H, *J* = 2.8 Hz), 1.56–1.68 (m, 2H), 2.97 (t, 2H, *J* = 5.2 Hz), 3.38–3.62 (m, 27H), 4.56–4.64 (m, 2H), 4.68–4.80 (m, 1H), 7.43 (d, 2H, *J* = 8.0 Hz), 7.80 (d, 2H, *J* = 8.0 Hz), 7.75–7.84 (bs, 3H), 8.29 (bs, 1H), 8.47 (t, 1H, *J* = 5.2 Hz), 9.18 (bs, 1H); *m/z* [M⁺ + 1] 661.1.

(*R*)-Roscovitine-linker Amine (**4b**)

(*R*)-Roscovitine-linker amine (**4b**) was synthesized with the same method as described for **4a** by using (*R*)-roscovitine-linker azide (**3b**).

(*R*)- or (*S*)-Roscovitine-agarose Matrices

Affi-Gel® 10 Gel (Bio-Rad) (5 ml bed volume) was rinsed with anhydrous dimethyl sulfoxide (Me₂SO) (3 × 10 ml) and transferred into a vial containing a solution of linker tethered compound **4a** or **4b** in Me₂SO (3 mM, 5 ml). The mixture was agitated at room temperature for 1 h in the presence of triethylamine (10 μl). The progress of the coupling reaction was monitored by LC-MS. Upon completion of the coupling, an excess amount of ethanolamine (50 μl) was added to block any unre-

acted groups that remain on the resin. The mixture was agitated for 10 h at room temperature. The resulting beads were washed with Me₂SO (10 ml × 3), phosphate-buffered saline (PBS) (3 × 10 ml), and stored in PBS (5 ml, with 0.05% NaN₃) at 4 °C until use.

Aminopurvalanol (NG-97)

Aminopurvalanol (NG-97) matrix was synthesized as described in Ref. 6.

Commercial Roscovitine Beads (Linker Attached at the Hydroxyl Substitution of Roscovitine)—This matrix was obtained from Calbiochem (catalog number 557361). They were used as described below for our original roscovitine beads (linker attached at the benzyl substitution of roscovitine).

Affinity Chromatography on Immobilized Roscovitine

Buffers

Homogenization Buffer—The homogenization buffer was 60 mM β-glycerophosphate, 15 mM *p*-nitrophenyl phosphate, 25 mM Mops (pH 7.2), 15 mM EGTA, 15 mM MgCl₂, 1 mM dithiothreitol, 1 mM sodium vanadate, 1 mM NaF, 1 mM phenylphosphate, 10 μg of leupeptin/ml, 10 μg aprotinin/ml, 10 μg of soybean trypsin inhibitor/ml, and 100 μM benzamide.

Bead Buffer—The bead buffer was 50 mM Tris (pH 7.4), 5 mM NaF, 250 mM NaCl, 5 mM EDTA, 5 mM EGTA, 0.1% Nonidet P-40, 10 μg/ml of leupeptin, aprotinin, and soybean trypsin inhibitor, and 100 μM benzamide.

Preparation of Extracts

Rat tissues were dissected and snap frozen until further use. Pork brains were obtained from a local slaughterhouse and directly homogenized and processed for affinity chromatography or stored at −80 °C prior to use. Tissues were weighed, homogenized, and sonicated in homogenization buffer (2 ml/g of material). Homogenates were centrifuged for 10 min at 14,000 × *g* at 4 °C. The supernatant was recovered, assayed for protein content (Bio-Rad protein assay), and immediately loaded batchwise on the affinity matrix.

Affinity Chromatography of Roscovitine-interacting Proteins

Just before use, 10 μl of packed roscovitine beads were washed with 1 ml of bead buffer and resuspended in 600 μl of this buffer. The cell or tissue extract supernatant (3 mg of total protein) or purified protein was then added; the tubes were rotated at 4 °C for 30 min. After a brief spin at 10,000 × *g* and removal of the supernatant, the beads were washed 4 times with bead buffer before addition of 60 μl of 2× Laemmli sample buffer. Following heat denaturation for 3 min, the bound proteins were analyzed by SDS-PAGE and Western blotting or silver staining as described below.

Electrophoresis and Western Blotting

Antibodies—Some antibodies were obtained from commercial sources: anti-CDK5 C-8 (Santa Cruz, Sc-173, 1:500, 1 h), anti-PSTAIRES (Sigma number P7962, 1:3000, 1 h), anti-ERK1 (Zymed Laboratories Inc. number 13-8600, 1:1000, 1 h), anti-ERK1/2 (Sigma number M7927, 1:4000, 1 h), anti-CDK2 (Santa Cruz, Sc-163, 1:500, 1 h), and anti-actin (Oncogene Research Products, CP01, 1:2000, 1 h). Anti-PDXK was generated by Eurogentec Europe (Double XP program). Two rabbits were immunized with a mixture of two human PDXK internal peptides: LLAWTHKHPNNLK (amino acids 241–253) and LRMVQSKRDIED-PEI (amino acids 291–305). The resulting antiserum (1:500, 1 h) cross-reacts with PDXK from a variety of species including mouse, rat, porcine, monkey, and human.

Electrophoresis and Western Blotting—Following heat denaturation for 3 min, the proteins bound to the roscovitine matrix were separated by 10% SDS-PAGE (0.7 mm thick gels) followed by immunoblotting analysis or silver staining using an Amersham SDS-PAGE silver staining kit. For immunoblotting, proteins were transferred to 0.45-μm nitrocellulose filters (Schleicher and Schuell). These were blocked with 5% low fat milk in Tris-buffered saline/Tween 20, incubated for 1 h with antibodies, and analyzed by Enhanced Chemiluminescence (ECL, Amersham).

MALDI-TOF Peptide Mapping Protein Identification

The protein bands were excised from a one-dimensional SDS-PAGE and digested in gel with trypsin as described previously (50). The resulting peptides were purified and concentrated on homemade nano-scale reversed phase disposable columns (51) prior to MALDI analysis using a M@LDI LR (Micromass, Manchester, UK). ProteinLynx Global

Server 2.0 (Micromass) software was used to search the SwissProt and nrdb sequence databases.

Protein Kinase Assays

The description of protein kinase preparation and assays is provided in the supplemental materials.

Pyridoxal Kinase Assay

PDXK was purified to homogeneity from sheep brain (53) or expressed in COS cells (see below). PDXK assays were run in an Uvikon 930 spectrophotometer equipped with a constant temperature cell holder maintained at 37 °C. PDXK activity was assayed by following the increase in absorption at 388 nm, at which pyridoxal 5'-phosphate has an absorption maximum. Assays were run, at 37 °C, in the presence of 70 mM potassium phosphate (pH 6.4), 0.05 mM ZnCl₂, 0.1 mM ATP, and 0.1 mM pyridoxal. The A₃₈₈ change was measured against a blank (same mixture of reagents but no enzyme). Reactions were performed in polymethylmethacrylate-disposable cuvettes. Addition of the substrates was used to start the reaction. The amount of PDXK was chosen to provide a linear reaction during the first 10 min of the reaction. Initial slope rates were used to calculate PDXK activities, which are expressed in ΔA₃₈₈/min/μl of PDXK or as percent of the maximal activity (measured in the absence of inhibitor). Me₂SO had no effect on PDXK activity at the highest concentration used (1%).

Pyridoxal 5'-Phosphate Level Determination in Erythrocytes

Blood was obtained from healthy volunteers, following informed, written consent, in accordance with the Declaration of Helsinki. Erythrocytes were separated from other blood components by centrifugation for 5 min at 2,500 × *g* and subsequent washings in PBS. One day before treatment, 2 × 10⁸ erythrocytes were seeded in RPMI 1640 (BioWhittaker) per experiment. The next day the cells were treated with (*R*)-roscovitine, (*S*)-roscovitine, or Me₂SO at the indicated concentrations and times. After treatment, the erythrocytes were harvested by centrifugation, snap frozen in dry ice, and stored at −80 °C until further analysis. Pyridoxal and pyridoxal 5'-phosphate levels were determined by cation exchange chromatography using recent improvements in extraction and detection methods (54). The erythrocyte pellet was suspended in 1 ml of water followed by 2 ml of 22.5% trichloroacetic acid. After centrifugation, the supernatant was transferred to a glass-stoppered centrifuge tube and extracted with 6 ml diethyl ether. A 0.5-ml aliquot of the aqueous layer was injected for analysis.

Expression of Human PDXK in COS Cells

COS6 cells were cultured in standard Dulbecco's modified Eagle's medium supplemented with 10% fetal calf serum, glutamine, and antibiotics. Transient transfections were performed in COS6 cells using Lipofectamine™ 2000 (Invitrogen) according to the manufacturer's instructions. In short, cells were plated at 70% confluence in 150-cm² flasks. Transfections was performed the next day using per flask: 40 μg of cesium chloride gradient-purified plasmid pCDM8-PKH combined with 100 μl of Lipofectamine™ in Opti-MEM® medium. As a control, a single flask was transfected with both 3 μg of pEGFP-NLS and 40 μg of pCDM8-PKH. 48 h later the control flask was examined for green fluorescent protein expression. In the case of more than 50% transfection efficiency, the non-green fluorescent protein flasks were harvested.

Co-crystallization of Roscovitine-Pyridoxal Kinase Complex

Pyridoxal kinase was purified from sheep brain as described by Kerry *et al.* (53). PDXK(*R*)-roscovitine complex crystals were obtained using the hanging drop vapor diffusion method at a constant temperature of 17 °C. The reservoir solution consisted of 1.4 M ammonium sulfate in 100 mM KH₂PO₄-K₂HPO₄ buffer (pH 8.2). Drops were composed of equal volumes of protein solution (10 mg/ml PDXK and 3 mM (*R*)-roscovitine) and reservoir solution. After incubation for about 1 month, suitable crystals were obtained (see accompanying paper (55) for a complete description of the crystallization procedures).

Cell Survival and Cell Proliferation Assays

Cell Culture

CDK2 null and wild type mouse embryonic fibroblasts (MEF) were generated from heterozygous CDK2 knock-out mice as described elsewhere (56). Cells were grown in Dulbecco's modified Eagle's medium + 10% calf serum. MEFs were immortalized following a 3T3 protocol and MEF lines used for the experiments (56).

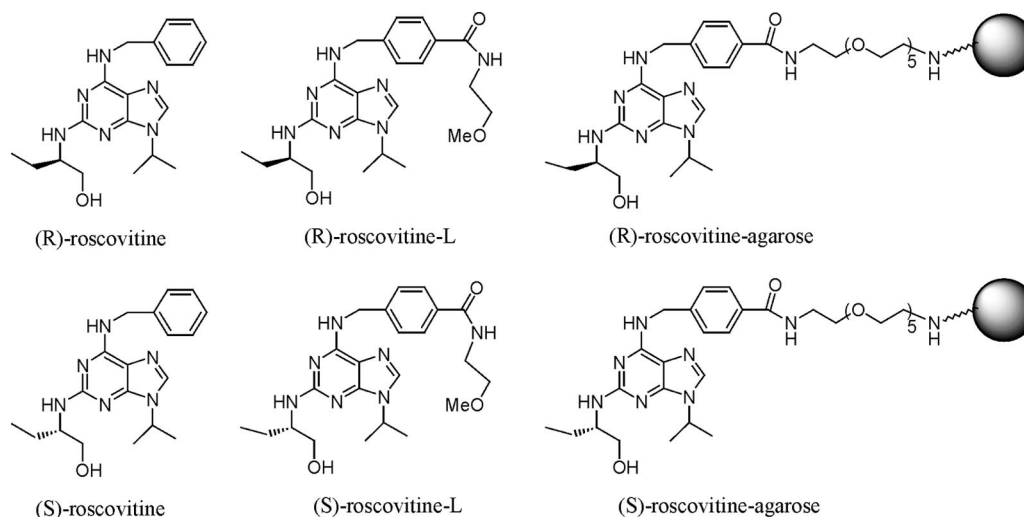


FIG. 1. Structure of roscovitine and analogs used in this study. (*R*- and (*S*)-Roscovitine, (*R*- and (*S*)-roscovitine-L (linker), and polyethylene glycol-immobilized (*R*- and (*S*)-roscovitine.

Cytotoxicity Assays

Compounds were tested in 96-well plates. Cells growing in a flask were harvested just before confluence, counted using a hemocytometer, and diluted with media to adjust the density to 5000 cells per well. The cells were allowed to recover for 24 h before adding the compounds. A “mother plate” with serial dilutions was prepared at 200 times the final concentrations in the culture from a 100 mM stock solution in pure Me₂SO. Final Me₂SO concentration did not exceed 0.5% in the culture media. The appropriate volume of the compound solution (usually 2 μl) was then automatically added (Beckman FX 96 tip) to the culture media. Old media was removed from cell cultures and replaced with 0.2 ml of media dosed with drug. Each concentration was assayed in triplicate. Two sets of control wells were left on each plate, containing either medium without drug or medium with the corresponding concentration of Me₂SO. A third control set was obtained with cells taken just before addition of the drugs (seeding control, number of cells at the start of the culture). Cells were exposed to the drugs for 96 h and washed twice with PBS before being fixed with 10% glutaraldehyde. Cells were then washed twice and stained with 0.5% crystal violet for 30 min. Finally they were extensively washed, solubilized with 15% acetic acid, and quantified by measuring the absorbance at 595 nm using a microplate reader (Bio-Rad).

Cell Cycle Analysis

Cells were seeded at low density (approximately 25%) in 10-cm dishes, grown during 24 h, then treated with the indicated agent. After 48 h exposure to various concentrations of roscovitine, cells were trypsinized, fixed with 70% methanol, and washed twice with PBS containing 0.1% fetal calf serum. After incubation in PBS supplemented with RNase (10 mg/ml) and propidium iodide (5 mg/ml) for 30 min, the DNA content was analyzed by FACSscan (56).

RESULTS

Protein Kinase Selectivity of Roscovitine—Roscovitine exists as two stereoisomers, (*R*)-roscovitine and (*S*)-roscovitine (Fig. 1). The (*R*)-isomer is slightly more active on CDKs (38, 40) (Fig. 2) and has been used in most biological studies. It has been selected for preclinical and clinical evaluations (44, 48).

To evaluate the selectivity of roscovitine, we tested (*R*)-roscovitine on the ProQinase selectivity panel (85 kinases), the Invitrogen SelectScreen™ kinase profiling panel (70 kinases), and the Cerep kinase selectivity panel (50 kinases). We also compiled previously published data (4, 39) and some unpublished results from our laboratory.² At present, a total of 151 protein kinases have been tested for their sensitivity to roscovitine (supplemental materials Table I). IC₅₀ values were below 1 μM for CDK1, CDK2, CDK5, CDK7, and CDK9 only. CDK4,

CDK6, and CDK8 were poorly if at all sensitive to roscovitine. Only a few kinases were sensitive to roscovitine in the 1–40 μM range (CaM kinase 2, CK1α, CK1δ, DYRK1A, EPHB2, ERK1, ERK2, FAK, and IRAK4). Most other kinases were insensitive to roscovitine. Based on supplemental materials Table I data, roscovitine appears as a reasonably selective kinase inhibitor. However, this panel only reflects 29.2% of the reported 518+ kinases of the human genome. In addition, roscovitine might target other proteins, beside protein kinases, which use ATP, GTP, or NAD.

Immobilized Roscovitine Matrix—An affinity chromatography approach, using roscovitine immobilized on a solid matrix, was therefore designed to purify the targets of roscovitine. Such a method has previously been applied successfully to purvalanol (6), paullones (7), indirubins (52), and hymenialdine (13). The crystal structure of roscovitine in complex with CDK2 (38) and CDK5 (34) shows that the benzyl ring substitution faces the outside of the ATP binding pocket of the kinases. This is where a polyethylene glycol extension was attached (Fig. 1). Addition of a linker on this site (leading to (*R*)- and (*S*)-roscovitine-L) did indeed not significantly modify the CDK1, CDK5, ERK1, ERK2, and DYRK1A inhibition properties (Fig. 2 and supplemental materials Table II). The linker allowed the covalent binding of roscovitine to agarose (Fig. 1). Both (*R*)-roscovitine- and (*S*)-roscovitine-agarose matrices were prepared as well as control beads (quenched with ethanolamine).

Affinity Purification of Roscovitine Targets—Extracts of biological material were prepared with homogenization buffer and incubated for 30 min, under constant rotation, at 4 °C, with control beads, (*R*)- or (*S*)-roscovitine-agarose beads, and purvalanol-agarose beads. After extensive washing with bead buffer, Laemmli sample buffer was added to the beads, and the bound proteins were analyzed by SDS-PAGE electrophoresis followed by silver staining or Western blotting with specific antibodies. A number of protein bands were also excised from the gel for identification either by microsequencing of internal tryptic peptides or by MALDI-TOF peptide mapping.

We first analyzed the roscovitine-binding proteins from porcine brain (Fig. 3). SDS-PAGE followed by silver staining revealed, besides the expected ERK1, ERK2, and CDK5, a 35-kDa protein that specifically bound to (*R*)-roscovitine-Sepharose (Fig. 3A). Microsequencing and Western blotting unequivocally identified this protein as PDXK. PDXK catalyzes the phosphorylation of pyridoxine, pyridoxal, and pyridoxamine to, respectively, pyridoxine 5'-phosphate,

² L. Meijer, unpublished data.

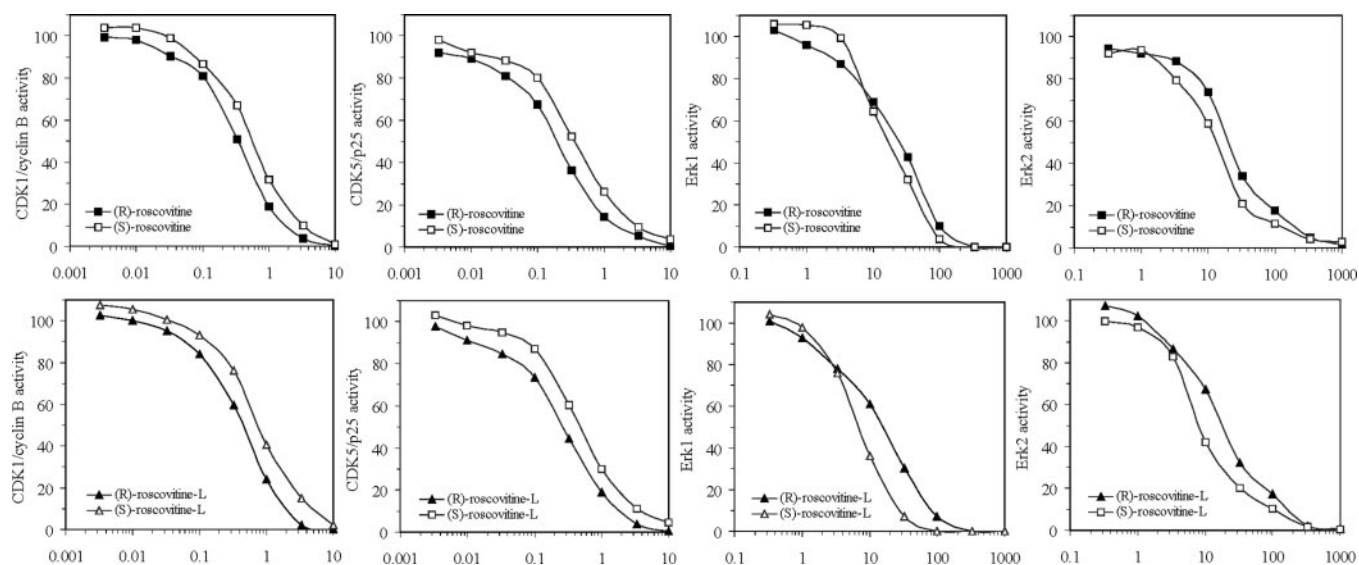


FIG. 2. Effects of both stereoisomers of roscovitine and roscovitine-L on the catalytic activity of some representative kinases. CDK1/cyclin B, CDK5/p25, ERK1, and ERK2 were assayed in the presence of increasing concentrations of (*R*)- and (*S*)-roscovitine (upper panels) and (*R*)- and (*S*)-roscovitine-L (lower panels). Kinase activities are expressed in % of maximal activity, *i.e.* measured in the absence of inhibitor.

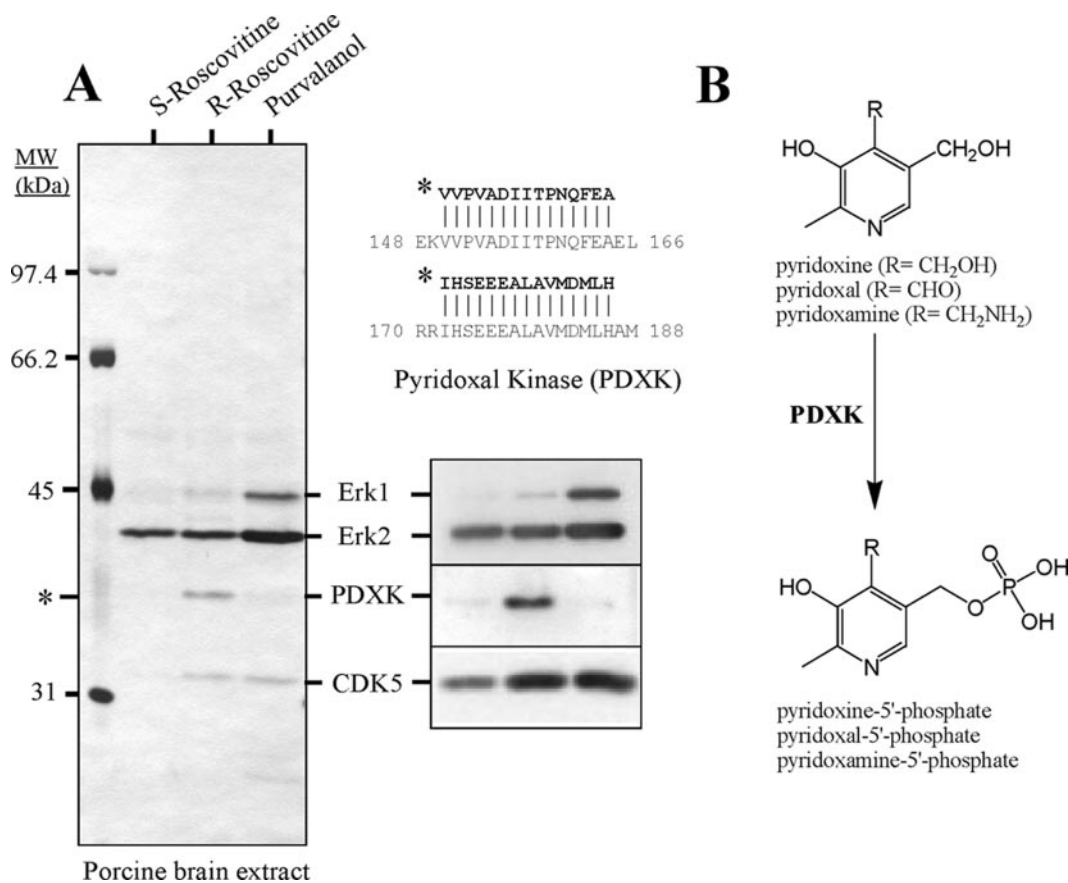
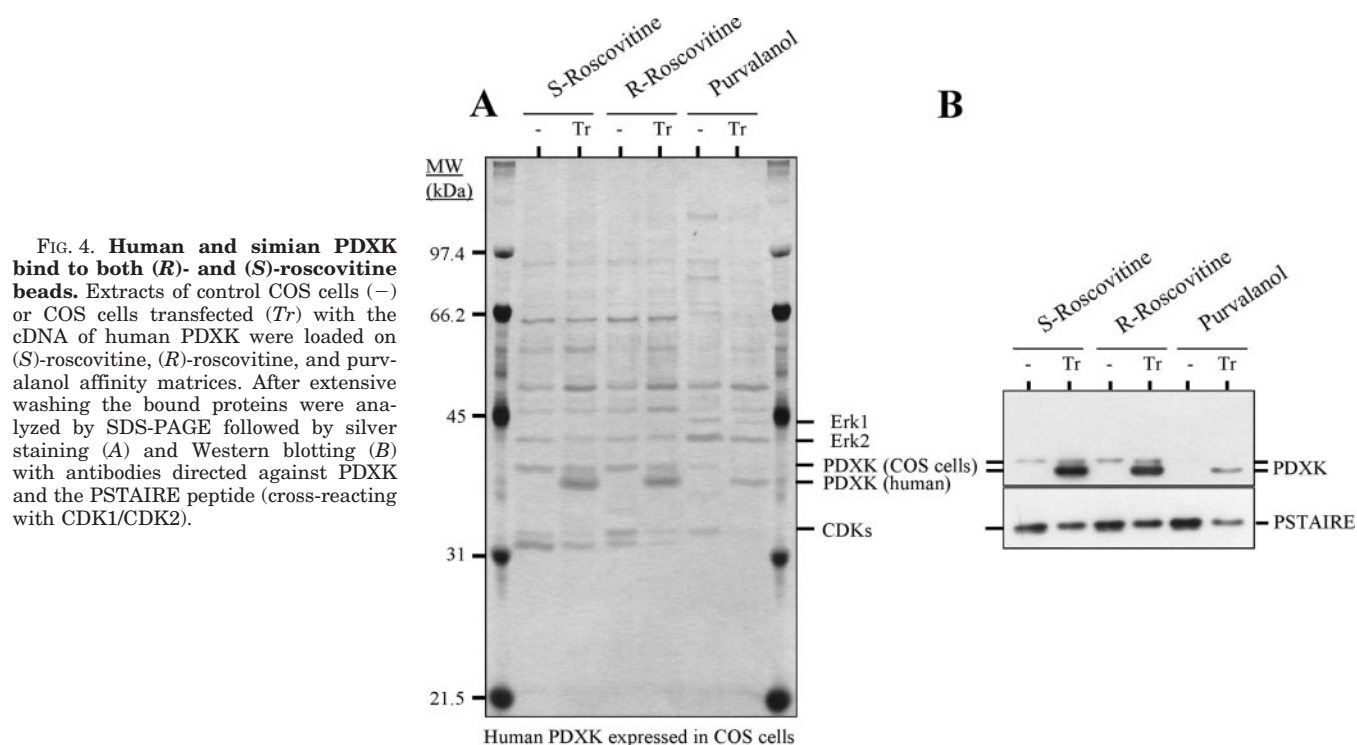


FIG. 3. Pyridoxal kinase binds to immobilized (*R*)-roscovitine. A, a porcine brain extract was loaded on immobilized (*S*)-roscovitine, (*R*)-roscovitine, and purvalanol. Beads were extensively washed, and the bound proteins were analyzed by SDS-PAGE followed by silver staining and Western blotting against CDK5, ERK1/ERK2, PDXK. Microsequencing of internal peptides of an unknown protein band (*) identified the protein as PDXK. B, the PDXK catalytic reaction.

pyridoxal 5'-phosphate, and pyridoxamine 5'-phosphate (Fig. 3B).

We further confirmed this interaction with recombinant human PDXK (53) transiently expressed in COS cells, a cell line derived from green monkey kidney. Cells were accumulated after PDXK expression, and extracted with homogenization buffer. Extracts were incubated with (*R*)-roscovitine, (*S*)-rosco-

vitine, and purvalanol-agarose beads. Analysis of the bound proteins by SDS-PAGE followed by silver staining and Western blotting shows that recombinant human PDXK binds equally well to (*R*)-roscovitine and (*S*)-roscovitine beads (Fig. 4). Furthermore, endogenous, COS cell-derived PDXK also binds to both matrices. PDXK from human 293 cells (data not shown) and from human erythrocytes (see below) also bind to both (*R*)-



and (*S*)-roscovitine matrices. Binding of CDK1 and CDK2 to roscovitine beads was monitored using an anti-PSTAIRE antibody (Fig. 1, *right*). Expression of PDXK results in reduced binding of CDKs, suggesting a competition for binding to roscovitine. PDXK may thus act as a sink for roscovitine and cells expressing high levels of PDXK might thus lose some sensitivity to roscovitine.

We next analyzed the roscovitine-binding proteins from various rat tissues (Fig. 5). Silver staining shows that the pattern of roscovitine-binding proteins varies from one tissue to another. However, some protein bands appear to be shared by many different tissues. For example, ERK1 and ERK2, identified by microsequencing and Western blotting, were found in all tissues but heart. One band (*) appeared to be preferentially purified on (*R*)-roscovitine beads *versus* (*S*)-roscovitine. It was particularly abundant in brain, liver, and kidney. Its identity as PDXK was confirmed by microsequencing in kidney and by Western blotting in various tissues, substantiating results obtained in porcine (Fig. 3) and sheep (not shown) brain tissues. CDK5 was present mostly, but by far not exclusively, in brain tissue. Various calmodulin-dependent kinase 2 isoforms were identified in various tissues. Casein kinase 1 α (CK1 α) was identified in kidney and is likely present in most tissues.

As this work was progressing a laboratory reagent company commercialized immobilized roscovitine beads (along with control beads, devoid of ligand). According to the manufacturer, roscovitine is bound to polyacrylamide beads through a 3-carbon spacer linker attached on the hydroxyl substitution of roscovitine (Fig. 6). As this area is facing the inside of the ATP binding pocket, this matrix could actually constitute a control matrix for our roscovitine matrix. Indeed we were unable to detect CDKs or PDXK on the commercial, hydroxyl-linked, roscovitine matrix loaded with extracts of either porcine brain or mouse fibroblasts, in contrast to our benzyl-linked roscovitine matrix (Fig. 6). Only very small amounts of ERK2 (porcine brain) and CDK1 (starfish oocytes) were detected on the commercial beads.

Roscovitine Targets PDXK: Competition with ATP, Pyridoxal but Not Pyridoxal 5'-Phosphate—Among the potential targets

of roscovitine, we selected to focus our investigation on the non-protein kinase target PDXK.

We first analyzed the effects of increasing the concentrations of ATP, pyridoxal, and pyridoxal 5'-phosphate in the brain extract, prior to and during incubation with (*R*)-roscovitine beads, on the binding of several protein targets (Fig. 7). Results show that ATP competes for binding of ERK1, ERK2, CDK5, and PDXK (Fig. 7A). Pyridoxal only competes with the binding of PDXK, but not of the protein kinases (Fig. 7B), whereas pyridoxal 5'-phosphate does not compete with PDXK binding (Fig. 7C). PDXK thus does not bind to roscovitine beads indirectly, *i.e.* through one of the protein kinases, but through a direct interaction. This is also supported by the binding of homogeneity purified PDXK to (*R*)-roscovitine-Sepharose (not shown). These results are also consistent with the PDXK/roscovitine co-crystal structures (see accompanying paper) (55) that show that roscovitine occupies the ATP-pyridoxal binding groove of PDXK (Fig. 8). Interestingly roscovitine is not directly binding at the ATP site, but at the pyridoxal site (Fig. 8). Yet, ATP competes with the binding of PDXK to roscovitine beads (Fig. 7A). The interaction of PDXK with ATP may thus either reduce the affinity of PDXK for roscovitine or enhance the affinity of PDXK for pyridoxal. We next tested the effects of roscovitine on the catalytic activity of either recombinant human PDXK expressed in COS cells or in purified native sheep brain PDXK (data not shown). The PDXK assay requires a 100 μ M ATP concentration and such high levels may prevent binding of roscovitine explaining why only very modest inhibition was observed at high concentrations (100 μ M) (data not shown).

We next analyzed the effects of roscovitine on the level of pyridoxal 5'-phosphate in human erythrocytes (Fig. 9). As these cells are known for their low content in vitamin B₆ and do not proliferate, we expected that roscovitine would have more detectable effects in this cellular model. First we verified that erythrocyte PDXK interacts with immobilized roscovitine (Fig. 9A). In contrast to PDXK from non-primate mammals, which only binds to (*R*)-roscovitine, human erythrocyte PDXK binds to both roscovitine isomers (Fig. 9A). Red blood cells were

FIG. 5. (R)- and (S)-Roscovitine-interacting proteins in various rat tissues. Extracts prepared from rat tissues were loaded on (R)- and (S)-roscovitine-agarose beads. After extensive washing the bound proteins were analyzed by SDS-PAGE followed by silver staining (*upper panel*) or Western blotting (*lower panels*) using antibodies directed against ERK1/ERK2, PDXK (*), and CDK5. In addition, several protein bands were excised from the gel and identified by MALDI-TOF peptide mapping. They are indicated in **bold letters**. CaMK2, calmodulin-dependent protein kinase.

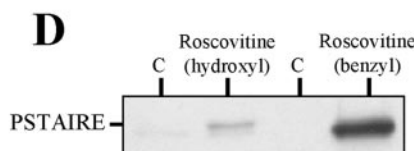
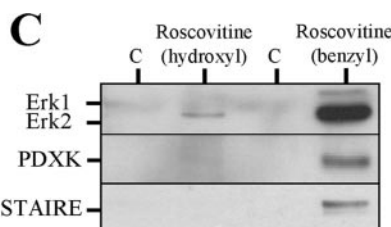
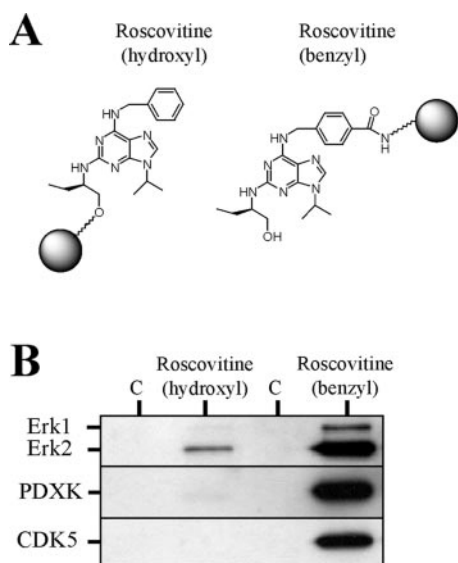
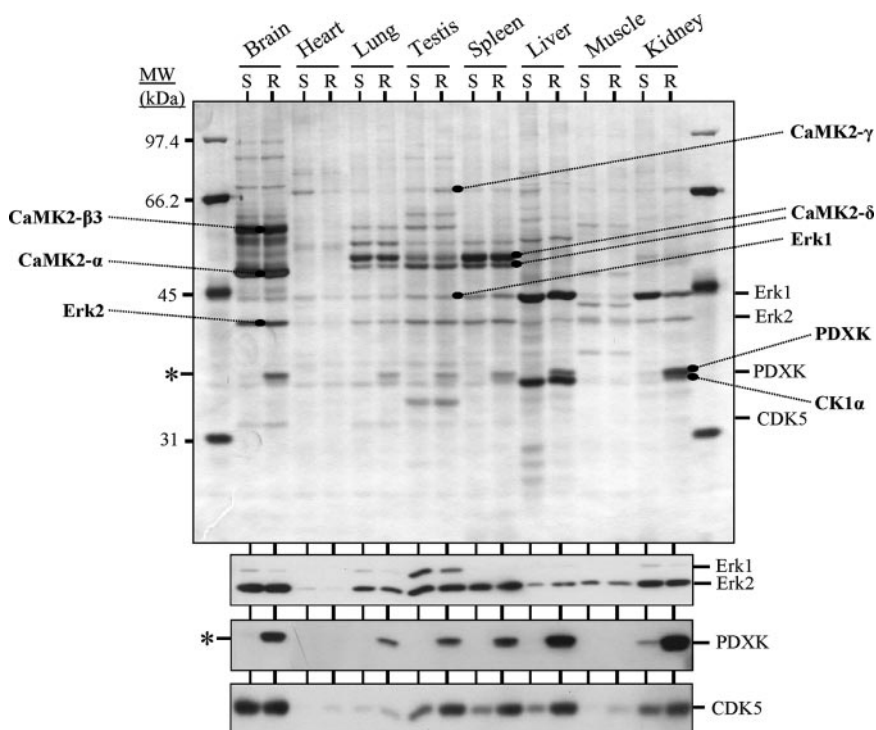


FIG. 6. CDKs, ERK1/2, and PDXK preferably bind to roscovitine immobilized through the benzyl ring. A, the structure of commercial roscovitine beads (linker attached at the hydroxyl substitution) and our roscovitine beads (linker attached at the benzyl substitution). Extracts from porcine brain (B), mouse embryonic fibroblasts (C), or starfish M phase oocytes (D) were loaded on either the commercial roscovitine beads, and their control beads (c), or to our (R)-roscovitine beads, and their control (c). The bound proteins were analyzed by SDS-PAGE followed by Western blotting using antibodies directed against ERK1/ERK2, PDXK, CDK5, and the PSTAIRE peptide (cross-reacting with CDK1, CDK2, and CDK3).

incubated with (R)-roscovitine, (S)-roscovitine (100 μM , final concentration), or vehicle (Me_2SO), in PBS and for various durations. Erythrocytes were extracted and their pyridoxal 5'-phosphate and pyridoxal levels were evaluated following purification by high performance liquid chromatography. Both (R)-roscovitine and (S)-roscovitine induced a significant decrease in the level of pyridoxal 5'-phosphate (Fig. 9B), whereas the overall level of pyridoxal remained constant (data not shown). The effect of both roscovitine isomers was dose-dependent (Fig. 9C).

Effects of Roscovitine on CDK2^{-/-} Mouse Embryonic Fibroblasts—An obvious target involved in the anti-proliferative and cytotoxic effects of roscovitine is CDK2. To evaluate the contribution of CDK2 inhibition to the cellular properties of roscovitine, we made use of CDK2^{-/-} MEFs and their corresponding CDK2^{+/+} control counterparts (56). First of all we verified that CDK2 was indeed absent from the roscovitine-interacting proteins that were affinity purified from CDK2^{-/-} cells (Fig. 10).

Other targets were present at equal levels in CDK2^{+/+} and CDK2^{-/-} cells (Fig. 10). Actin was found to bind consistently to all beads. MEFs were then exposed for 96 h to a range of (R)- and (S)-roscovitine concentrations. The extent of cell survival was evaluated using an 4,5-dimethylthiazol-2-yl-2,5-diphenyltetrazolium bromide assay (Fig. 11A). Dose-response curves show that IC₅₀ values are 26.0 μM (CDK2^{+/+}) and 50.0 μM (CDK2^{-/-}) for (R)-roscovitine, and 25.0 μM (CDK2^{+/+}) and 38.0 μM (CDK2^{-/-}) for (S)-roscovitine (average of three independent determinations made in triplicates). Thus, (S)-roscovitine is essentially as potent as (R)-roscovitine, and CDK2^{-/-} MEFs are only about 1.5–2-fold less sensitive to roscovitine than CDK2^{+/+}, suggesting that CDK2 inhibition accounts for only a fraction of the cytotoxic effects of roscovitine and that other targets are involved. We next analyzed the cell cycle distribution of CDK2^{+/+} and CDK2^{-/-} MEFs after a 48-h exposure to (R)-roscovitine or (S)-roscovitine (Fig. 11B). The results are quite striking: wild type MEFs accumulate in S phase as a

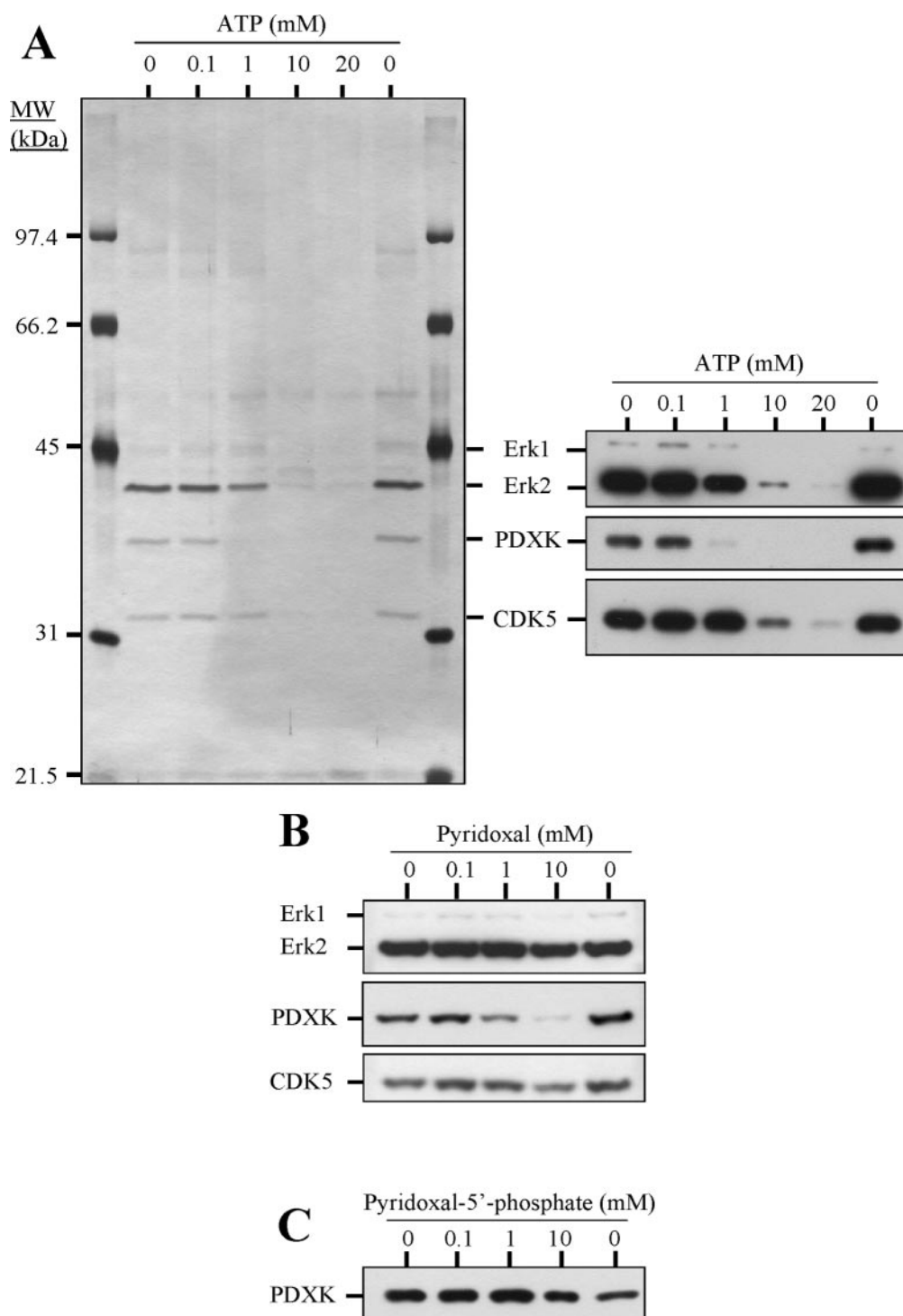


FIG. 7. ATP prevents the binding of PDXK, ERK1/2, and CDK5 to immobilized roscovitine (A), pyridoxal only inhibits PDXK binding (B), whereas pyridoxal 5'-phosphate has no effect (C). Porcine brain extracts were supplemented with increasing concentrations of ATP (A), pyridoxal (B), or pyridoxal 5'-phosphate (C), prior to loading on (*R*)-roscovitine beads. The bound proteins were analyzed by SDS-PAGE followed by silver staining (A, left) and Western blotting (A, right; B and C) using antibodies directed against ERK1/ERK2, PDXK, and CDK5.

result of exposure to roscovitine, whereas the absence of CDK2 completely prevents this accumulation in S phase. No difference was observed between the two stereoisomers of roscovitine (data not shown), suggesting that roscovitine-induced cytotoxicity does not involve an interaction with PDXK.

DISCUSSION

After G protein-coupled receptors, protein kinases constitute the second class of drug discovery screening targets. Among

protein kinases CDKs represent attractive targets because they are involved in cancers, neurodegenerative diseases, and viral infections. As one of the first apparently selective CDK inhibitors, roscovitine has been used in many fundamental research studies to support the involvement of CDKs in various cellular processes. In a more applied way, (*R*)-roscovitine is being investigated as a potential therapeutic agent. Roscovitine is frequently referred to as a "specific CDK inhibitor," yet what we knew about its specificity was essentially based on its *in vitro* effects on less than 50 kinases (4, 39) and on multiple

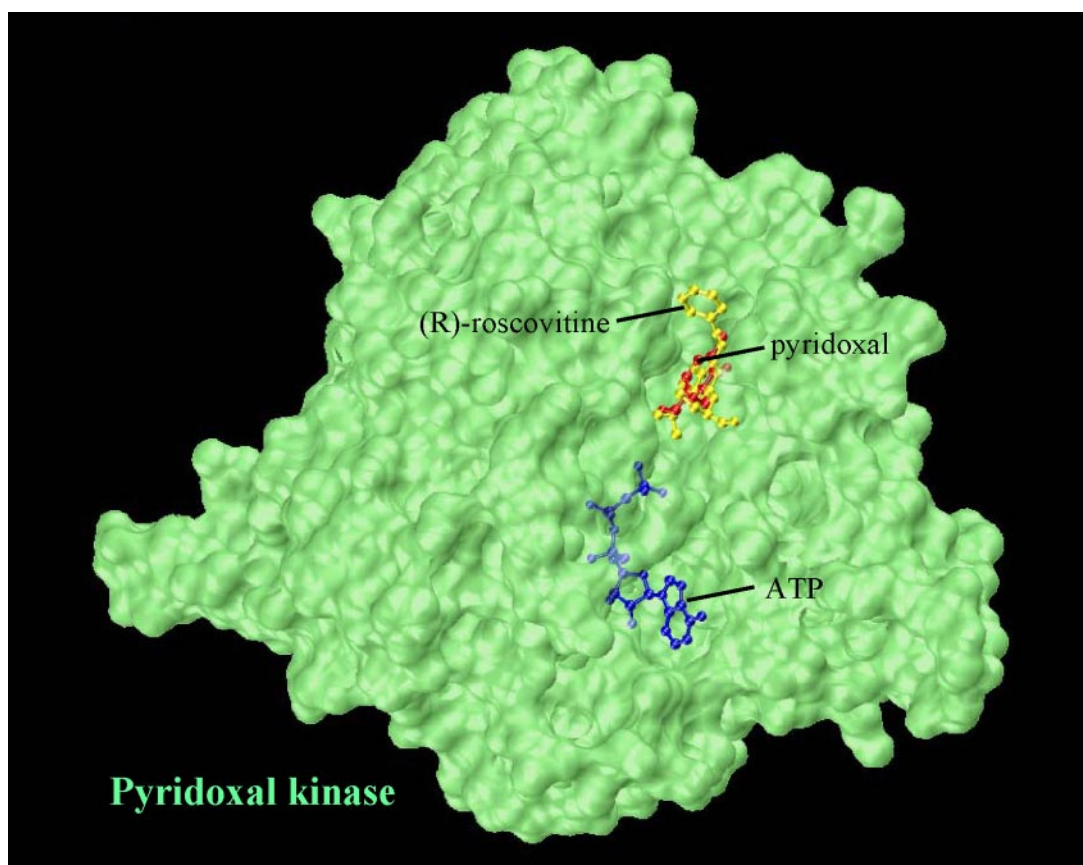


FIG. 8. Superimposition of the crystal structures of PDXK in complex with (*R*)-roscovitine, an ATP analog or pyridoxal. The overall view of PDXK (green) shows that (*R*)-roscovitine (yellow) binds at the site of pyridoxal (red) rather than at the site of ATP (blue).

cellular effects apparently consistent with the expected inhibition of CDKs. The purpose of this work was thus to characterize further the selectivity of roscovitine using several approaches.

Targets of Roscovitine

Protein Kinases—Four approaches confirm a rather good selectivity of roscovitine for a limited number of protein kinases: (i) the selectivity panel (supplemental materials) now expands the number of tested kinases to 151, in fact only 29.2% of the human kinome; (ii) the second approach, affinity chromatography, did not uncover any new protein kinase targets (except CK1); (iii) a triple hybrid yeast system, using (*R*)-roscovitine coupled to methotrexate as a bait (17), revealed that purvalanol, although more potent as a kinase inhibitor, is less selective than roscovitine, as previously noticed by screening on kinase panels (4, 39); (iv) a recent kinase specificity assay based on an *in vitro* quantitative competition method on 119 kinases (18) recently showed the rather good selectivity of roscovitine; it revealed interaction with and suggested inhibition of CK1 and CLK. Altogether these four independent methods show that a rather limited set of protein kinases are targeted by roscovitine, CDK1, -2, -5, -7, and -9 being the most sensitive kinases at present.

Pyridoxal Kinase—The affinity chromatography approach reveals an unexpected, non-protein kinase target for roscovitine, PDXK. The crystal structures of PDXK in complex with an ATP analog, with pyridoxal (57, 58), and with (*R*)-roscovitine (55), have been instrumental in understanding how (*R*)-roscovitine binds to PDXK. The structure of the PDXK-(*R*)-roscovitine complex reveals that the interaction occurs at the pyridoxal-binding site, rather than at the ATP-binding site as initially expected (Fig. 8). Although (*R*)-roscovitine beads bind PDXK from all biological sources tested, (*S*)-roscovitine beads do not

bind PDXK from mice, rat, pork, and sheep tissues. However, (*S*)-roscovitine beads bind PDXK from monkey and human sources, as well as recombinant human PDXK expressed in COS or HEK293 cells (Fig. 4). We are currently investigating the molecular reasons that account for these phylogenetical differences in PDXK interaction with roscovitine. Despite the interaction of roscovitine with PDXK, its effects on the catalytic activity of PDXK are rather limited. This might be explained by the potent competition exerted by ATP on PDXK binding of roscovitine (Fig. 7A). During the PDXK assay, the ATP concentration (100 μ M) might be sufficient to compete roscovitine out, therefore resulting in a weak effect on PDXK activity.

The Causes of the Effects of Roscovitine on Cell Proliferation

Some of the cellular effects of roscovitine are clearly because of CDK inhibition. This is demonstrated in the CDK2^{-/-} MEFs experiments (Figs. 10 and 11): (i) the absence of CDK2 indeed leads to a 1.5–2-fold reduction of the effects of roscovitine on cell survival; (ii) the cell cycle distribution (accumulation in S phase) in roscovitine-treated MEFs is highly dependent on the presence of CDK2. However, some of the effects of roscovitine on cell survival are clearly due to interaction with alternative, unidentified targets, as they occur in CDK2^{-/-} cells (Fig. 10A). As we have seen with the CDK inhibitor purvalanol (7), inhibition of alternative targets such as ERK1/2 contributes to the cellular effects of roscovitine.

Three arguments support the view that interaction of (*R*)-roscovitine with PDXK does not dominantly contribute to its anti-proliferative and pro-apoptosis effects: (i) the two roscovitine isomers have rather similar effects on rodent cells (survival dose-response curves and cell cycle distribution), although only the (*R*)-roscovitine isomer binds PDXK from

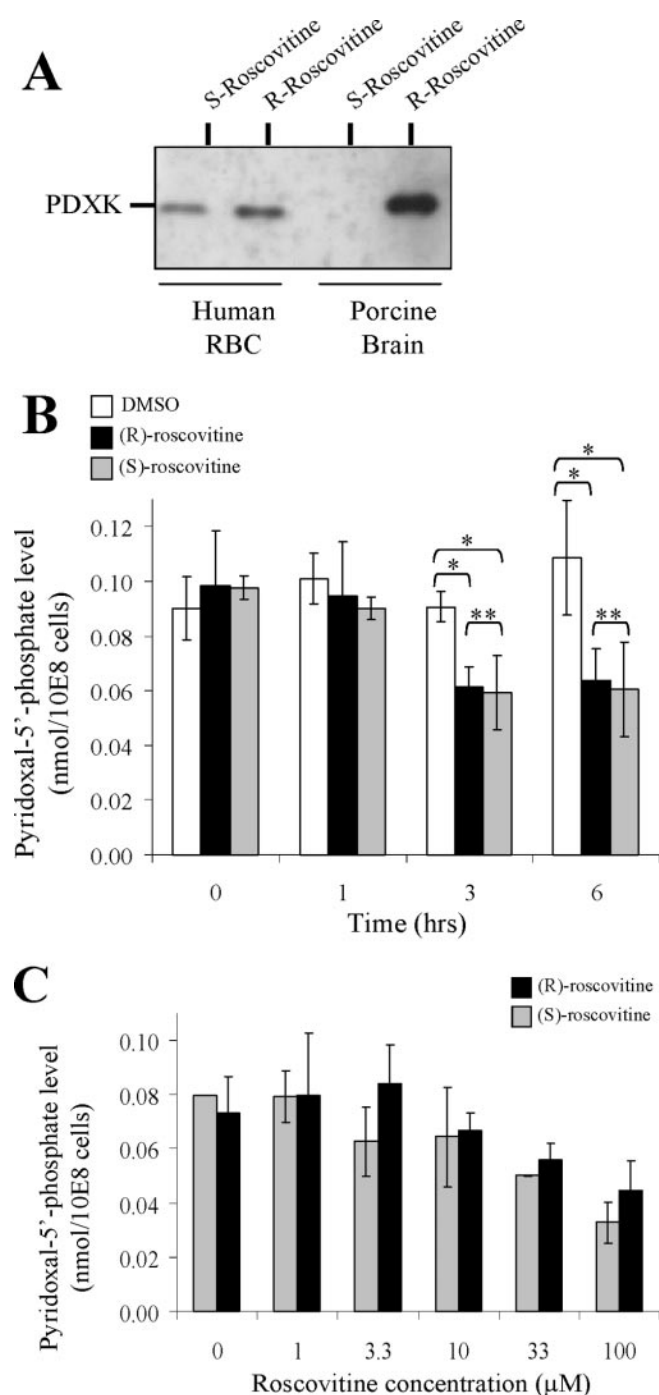


FIG. 9. Roscovitine treatment reduces the level of pyridoxal 5'-phosphate in human erythrocytes. *A*, extracts prepared from human erythrocytes and porcine brain were loaded on (*R*- and (*S*-roscovitine- agarose beads. After extensive washing the bound proteins were analyzed by SDS-PAGE followed by Western blotting using antibodies directed against PDXK. *B*, human erythrocytes were incubated for various durations with 100 μM (*R*-roscovitine or (*S*-roscovitine, or vehicle (Me_2SO). Erythrocytes were then processed for analysis of pyridoxal 5'-phosphate levels (average of three determinations). Student's *t* test analysis of the results revealed either a significant difference (*, $p < 0.05$) between control and roscovitine-treated or no significant difference (**, $p > 0.7$) between (*R*- and (*S*-roscovitine treatment. *C*, human erythrocytes were incubated for 6 h with various concentrations of (*R*-roscovitine or (*S*-roscovitine and then processed for analysis of pyridoxal 5'-phosphate levels.

MEF extracts (Figs. 10 and 11); (ii) the CDK inactive N⁶-methyl-(*R*-roscovitine, which still interacts with PDXK, has much reduced anti-proliferative or pro-apoptotic activity (data not shown); (iii) the sensitivity to (*R*-roscovitine of

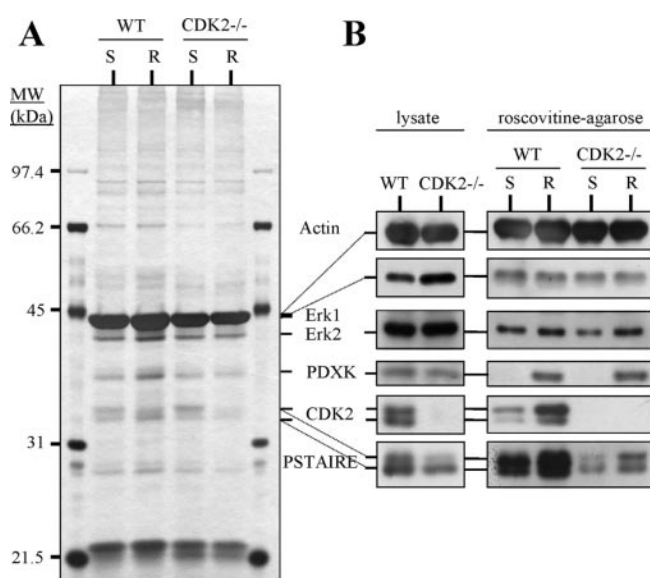


FIG. 10. Roscovitine-binding proteins of CDK2^{+/+} and CDK2^{-/-} mouse embryonic fibroblasts. Extracts prepared from wild-type (*WT*) or CDK2^{-/-} MEFs were loaded on (*R*- and (*S*-roscovitine-agarose beads. After extensive washing, the bound proteins were analyzed by SDS-PAGE followed by silver staining (*A*) or Western blotting (*B*) using antibodies directed against actin, ERK1/ERK2, PDXK, CDK2, and the PSTAIRE peptide.

HEK293 cells overexpressing PDXK is not substantially modified when compared with control HEK293 cells (data not shown). We plan to complement these experiments with the expression of dominant-negative PDXK and with selective interference RNA. Nevertheless, we cannot completely rule out contribution of the PDXK/roscovitine interaction in anti-proliferative effects of roscovitine as, under some circumstances (Fig. 9), (*R*-roscovitine is able to reduce the level of pyridoxal 5'-phosphate. At present the combined effect of (*R*-roscovitine on protein kinases such as CDKs and ERKs remains the most likely cause of its anti-proliferative and pro-apoptotic effects.

The Causes of Effects of Roscovitine on Neuronal Cells

PDXK catalyzes the formation of vitamin B₆, a co-factor of at least 140 enzymes, such as aminotransferases and decarboxylases, many of which are involved in amino acid and neurotransmitter metabolism (reviews in Refs. 59 and 60). Consequently interference with PDXK is expected to have profound effects on neuronal cells, in particular on the levels of GABA, serotonin, and dopamine. As a matter of fact, it was recently shown that loss of the three PAR bZip transcription factors down-regulates brain PDXK expression, leads to reduction in the levels of pyridoxal 5'-phosphate, serotonin, and dopamine, and results in epilepsy in animal models (61). This was recently substantiated in man (62), where inactivating mutations in the pyridoxine-5'-phosphate oxidase led to reduced pyridoxal phosphate-dependent enzymes and the neonatal epileptic encephalopathy syndrome. Seizures, however, ceased with administration of pyridoxal phosphate. Although roscovitine has a limited capability to pass the blood-brain barrier, the interaction with neuronal PDXK issue should therefore be seriously considered. As discussed above, it is possible that roscovitine only binds PDXK in the absence of ATP, and therefore, does not prevent its activity, and, consequently, does not reduce the intracellular pyridoxal 5'-phosphate level significantly in most tissues (erythrocytes being an exception). Nevertheless, PDXK may still be able to trap roscovitine, thereby reducing its effects on other targets such as CDK5. If this were the case, roscovitine

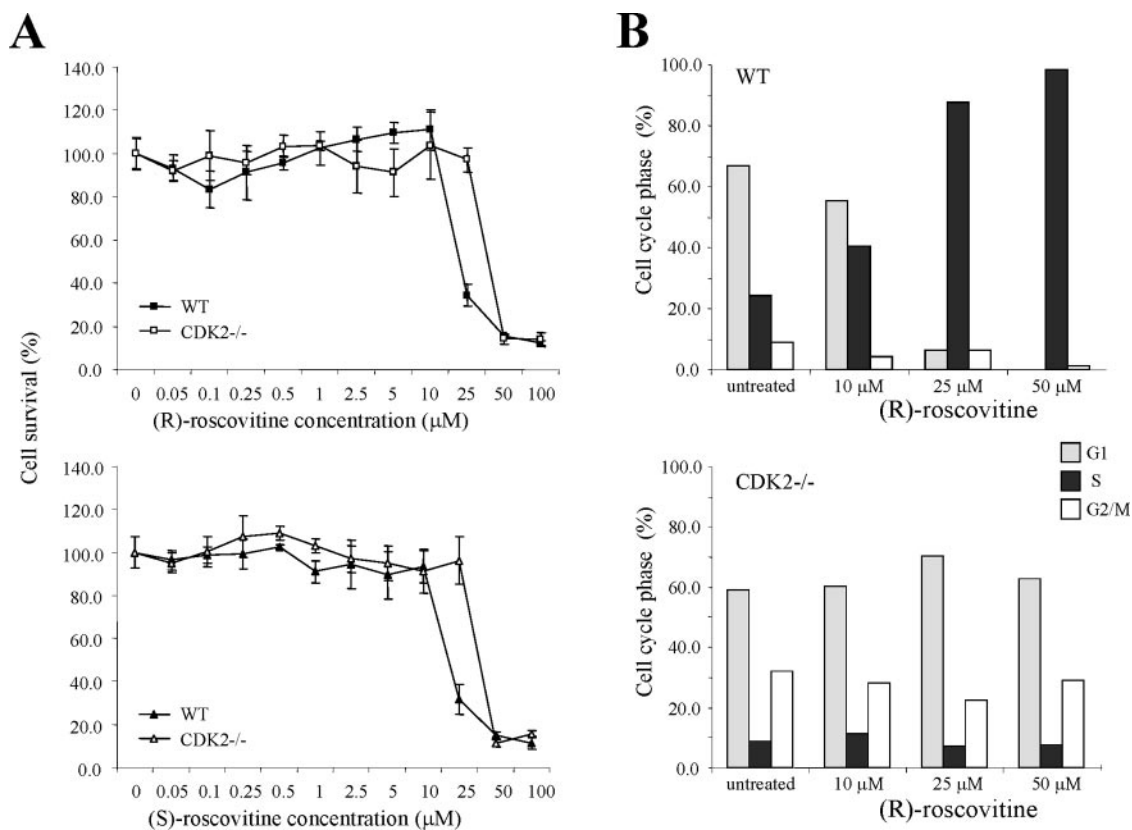


FIG. 11. The cellular effects of (R)- and (S)-roscovitine on survival (A) and cell cycle distribution of CDK2^{+/+} and CDK2^{-/-} mouse embryonic fibroblasts. Increasing concentrations of (R)-roscovitine (A and B) and (S)-roscovitine (A) were added to wild-type (WT) or CDK2^{-/-} MEFs. Cell survival (A) was estimated by a 4,5-dimethylthiazol-2-yl-2,5-diphenyltetrazolium bromide assay after 96 h of exposure to roscovitine. Student's *t* test analysis of the results (three independent experiments) revealed a significant difference between wild-type (WT) and CDK2^{-/-} MEFs for both IC₅₀ values of (R)-roscovitine ($p < 0.05$) and (S)-roscovitine ($p < 0.005$). B, cell cycle distribution in the G₁, S, and G₂/M cell cycle phases was analyzed by fluorescence-activated cell sorter analysis after 48 h (representative of two experiments).

derivatives that do not bind PDXK might be both more active and safer than (R)-roscovitine for neuronal applications. These compounds are currently being synthesized.

In summary we have extensively investigated the targets of (R)-roscovitine, a frequently used pharmacological inhibitor of CDKs. To our knowledge, roscovitine has been tested on the largest panel of kinases (151) ever used to characterize a kinase inhibitor. Selectivity for CDK1, -2, -5, -7, and -9 was confirmed, although a few other kinases are inhibited in the 1–40 μM IC₅₀ range. Affinity chromatography on immobilized roscovitine confirmed that the drug binds only a few protein kinases but also PDXK. Comparison of the binding modes of (R)-roscovitine with its protein kinase targets (CDK2 and CDK5) and with a non-protein kinase “off-target” (PDXK) should provide clues for the synthesis of roscovitine-derived, PDXK- or CDK-selective inhibitors. Finally we analyzed the effects of roscovitine on CDK2-depleted cells. Despite the absence of this main target, cells remain quite sensitive to roscovitine, suggesting that the effects of the drug on cell proliferation and survival originates from the inhibition of multiple kinase targets.

Acknowledgments—We thank Dr. J. E. Allende for recombinant CK1α, Dr. W. Becker for the DYRK1A and DYRK3 clones, Dr. M. Cobb for ERK1/2, Dr. V. Catros for rat tissues, Dr. A. Donella for Lyn tyrosine kinase, Dr. S. Facchin for pID261, Dr. H. Fisk and Dr. M. Winey for the Mps1 data, Dr. C. Gambacorti for ALK tyrosine kinase, and Dr. J. Wang for the CDK5 and p25 clones. We are very grateful to D. Lasky, Dr. T. Turek-Etienne, Dr. C. Armstrong, and M. Krueger (Invitrogen) for providing the data obtained with (R)-roscovitine by the Invitrogen SelectScreen™ Kinase Profiling Service and to Cerep for running (R)-roscovitine on its kinase selectivity panel. Special thanks are extended to the Experimental Oncology Group at CNIO (Dr. Barbacid) for the CDK2^{-/-} MEFs.

REFERENCES

- Cohen, P. (2002) *Nat. Rev. Drug Discovery* **1**, 309–315
- Fischer, P. M. (2004) *Curr. Med. Chem.* **11**, 1563–1583
- Davies, S. P., Reddy, H., Caivano, M., and Cohen, P. (2000) *Biochem. J.* **351**, 95–105
- Bain, J., McLauchlan, H., Elliott, M., and Cohen, P. (2003) *Biochem. J.* **371**, 199–204
- Daub, H., Godl, K., Brehmer, D., Klebl, B., and Müller, G. (2004) *Assay Drug Dev. Technol.* **2**, 215–224
- Knockaert, M., Gray, N., Damiens, E., Chang, Y. T., Grellier, P., Grant, K., Fergusson, D., Mottram, J., Soete, M., Dubremetz, J. F., LeRoch, K., Doerig, C., Schultz, P. G., and Meijer, L. (2000) *Chem. Biol.* **7**, 411–422
- Knockaert, M., Viking, K., Schmitt, S., Leost, M., Mottram, J., Kunick, C., and Meijer, L. (2002) *J. Biol. Chem.* **277**, 25493–25501
- Knockaert, M., Lenormand, P., Gray, N., Schultz, P., Pouyssegur, J., and Meijer, L. (2002) *Oncogene* **21**, 6413–6424
- Godl, K., Wissing, J., Kurtenbach, A., Habenberger, P., Blencke, S., Gutbrod, H., Salassidis, K., Stein-Gerlach, M., Missio, A., Cotton, M., and Daub, H. (2003) *Proc. Natl. Acad. Sci. U. S. A.* **100**, 15424–15439
- Lolli, G., Thaler, F., Valsasina, B., Roletto, F., Knapp, S., Uggeri, M., Bachi, A., Mafafora, V., Storici, P., Stewart, A., Kalisz, H. M., and Isacchi, A. (2003) *Proteomics* **3**, 1287–1298
- Shima, D., Yugami, M., Tatsuno, M., Wada, T., Yamaguchi, Y., and Handa, H. (2003) *Genes Cells* **8**, 215–223
- Brehmer, D., Godl, K., Zech, B., Wissing, J., and Daub, H. (2004) *Mol. Cell Proteomics* **3**, 490–500
- Wan, Y., Hur, W., Cho, C. Y., Liu, Y., Adrian, F. J., Lozach, O., Bach, S., Mayer, T., Fabbro, D., Meijer, L., and Gray, N. S. (2004) *Chem. Biol.* **11**, 247–259
- Knockaert, M., and Meijer, L. (2002) *Biochem. Pharmacol.* **64**, 819–825
- Valsasina, B., Kalisz, H. M., and Isacchi, A. (2004) *Expert Rev. Proteomics* **1**, 303–315
- Sche, P. P., McKenzie, K. M., White, J. D., and Austin, D. J. (1999) *Chem. Biol.* **6**, 707–716
- Becker, F., Murthi, K., Smith, C., Come, J., Costa-Roldan, N., Kaufmann, C., Hanke, U., Degenhart, C., Baumann, S., Wallner, W., Huber, A., Dedier, S., Dill, S., Kinsman, D., Hediger, M., Bockovich, N., Meier-Ewert, S., Kluge, A. F., and Kley, N. (2004) *Chem. Biol.* **11**, 211–223
- Fabian, M. A., Biggs, W. H., Treiber, D. K., Atteridge, C. E., Azimioara, M. D., Benedetti, M. G., Carter, T. A., Ciceri, P., Edeen, P. T., Floyd, M., Ford, J. M., Galvin, M., Gerlach, J. L., Grotzfeld, R. M., Herrgard, S., Insko, D. E., Insko, M. A., Lai, A. G., Lelias, J. M., Mehta, S. A., Milanov, Z. V., Velasco,

- A. M., Wodicka, L. M., Patel, H. K., Zarrinkar, P. P., and Lockhart, D. J. (2005) *Nat. Biotechnol.* **23**, 329–336
19. Kung, C., Kenski, D. M., Dickerson, S. H., Howson, R. W., Kuyper, L. F., Madhani, H. D., and Shokat, K. M. (2005) *Proc. Natl. Acad. Sci. U. S. A.* **102**, 3587–3592
 20. Malumbres, M., and Barbacid, M. (2001) *Nat. Rev. Cancer* **1**, 222–231
 21. Cruz, J. C., and Tsai, L. H. (2004) *Curr. Opin. Neurobiol.* **14**, 390–394
 22. Borgne, A., and Golsteyn, R. M., (2003) in *Progress in Cell Cycle Research* (Meijer, L., Jézéquel, A., and Roberge, M., eds) pp. 453–459, Roscoff, France
 23. Garriga, J., and Grana, X. (2004) *Gene (Amst.)* **337**, 15–23
 24. Malumbres, M., Ortega, S., and Barbacid, M. (2000) *Biol. Chem.* **381**, 827–838
 25. Vermeulen, K., Van Bockstaele, D. R., and Berneman, Z. N. (2003) *Cell Prolif.* **36**, 131–149
 26. Schang, L. M. (2004) *Biochim. Biophys. Acta* **1697**, 197–209
 27. Tsai, L. H., Lee, M. S., and Cruz, J. (2004) *Biochim. Biophys. Acta* **1697**, 137–142
 28. Smith, P. D., Crocker, S. J., Jackson-Lewis, V., Jordan-Sciutto, K. L., Hayley, S., Mount, M. P., O'Hare, M. J., Callaghan, S., Slack, R. S., Przedborski, S., Anisman, H., and Park, D. S. (2003) *Proc. Natl. Acad. Sci. U. S. A.* **100**, 13650–13655
 29. Smith, P. D., O'Hare, M. J., and Park, D. S. (2004) *Trends Mol. Med.* **10**, 445–451
 30. Zhang, M., Li, J., Chakrabarty, P., Bu, B., and Vincent, I. (2004) *Am. J. Pathol.* **165**, 843–853
 31. Wang, J., Liu, S. H., Fu, Y. P., Wang, J. H., and Lu, Y. M. (2003) *Nat. Neurosci.* **6**, 1039–1047
 32. Knockaert, M., Greengard, P., and Meijer, L. (2002) *Trends Pharmacol. Sci.* **23**, 417–425
 33. Noble, M. E., Endicott, J. A., and Johnson, L. N. (2004) *Science* **303**, 1800–1805
 34. Mapelli, M., Massimiliano, L., Crovace, C., Seeliger, M., Tsai, L. H., Meijer, L., and Musacchio, A. (2005) *J. Med. Chem.* **48**, 671–679
 35. Haesslein, J. L., and Jullian, N. (2002) *Curr. Top. Med. Chem.* **2**, 1035–1048
 36. Meijer, L., and Raymond, E. (2003) *Acc. Chem. Res.* **36**, 417–425
 37. Vesely, J., Havlicek, L., Strnad, M., Blow, J. J., Donella-Deana, A., Pinna, L., Letham, D. S., Kato, J. Y., Détivaud, L., Leclerc, S., and Meijer, L. (1994) *Eur. J. Biochem.* **224**, 771–786
 38. Azevedo, W. F., Leclerc, S., Meijer, L., Havlicek, L., Strnad, M., and Kim, S. H. (1997) *Eur. J. Biochem.* **243**, 518–526
 39. Meijer, L., Borgne, A., Mulner, O., Chong, J. P., Blow, J. J., Inagaki, N., Inagaki, M., Delcros, J. G., and Moulinoux, J. P. (1997) *Eur. J. Biochem.* **243**, 527–536
 40. Wang, S., McClue, S. J., Ferguson, J. R., Hull, J. D., Stokes, S., Parsons, S., Westwood, R., and Fischer, P. M. (2001) *Tetrahedron Asymmetry* **12**, 2891–2894
 41. Gray, N., Wodicka, L., Thunnissen, A. M., Norman, T., Kwon, S., Espinoza, F. H., Morgan, D. O., Barnes, G., Leclerc, S., Meijer, L., Kim, S. H., Lockhart, D. J., and Schultz, P. G. (1998) *Science* **281**, 533–538
 42. Chang, Y. T., Gray, N. G., Rosania, G. R., Sutherlin, D. P., Kwon, S., Norman, T. C., Sarohia, R., Leost, M., Meijer, L., and Schultz, P. G. (1999) *Chem. Biol.* **6**, 361–375
 43. Pippin, J. W., Qu, Q., Meijer, L., and Shankland, S. J. (1997) *J. Clin. Investig.* **100**, 2512–2520
 44. McClue, S. J., Blake, B., Clarke, R., Cowan, A., Cummings, L., Fischer, P. M., MacKenzie, M., Melville, J., Stewart, K., Wang, S., Zhelev, N., Zheleva, N., and Lane, D. P. (2002) *Int. J. Cancer* **102**, 463–468
 45. Raynaud, F. I., Fischer, P. M., Nutley, B. P., Goddard, P. M., Lane, D. P., and Workman, P. (2003) *Mol. Cancer Ther.* **3**, 353–362
 46. Gherardi, D., D'Agati, V., Chu, T. H., Barnett, A., Gianella-Borradori, A., Gelman, I. H., and Nelson, P. J. (2004) *J. Am. Soc. Nephrol.* **15**, 1212–1222
 47. Zhang, G. J., Safran, M., Wei, W., Sorensen, E., Lassota, P., Zhelev, N., Neuberg, D. S., Shapiro, G., and Kaelin, W. G., Jr. (2004) *Nature Med.* **10**, 643–648
 48. De la Motte, S., and Gianella-Borradori, A. (2004) *Int. J. Clin. Pharm. Ther.* **42**, 232–239
 49. Clough, J. (2002) *Drug Discovery Today* **7**, 789–790
 50. Shevchenko, A., Wilm, M., Vorm, O., and Mann, M. (1996) *Anal. Chem.* **68**, 850–858
 51. Gobom, J., Nordhoff, E., Mirgorodskaya, E., Ekman, R., and Roepstorff, P. (1999) *J. Mass Spectrom.* **34**, 105–116
 52. Meijer, L., Skaltsounis, A. L., Magiatis, P., Polychronopoulos, P., Knockaert, M., Leost, M., Ryan, X. P., Vonica, C. D., Brivanlou, A., Dajani, R., Tarricone, A., Musacchio, A., Roe, S. M., Pearl, L., and Greengard, P. (2003) *Chem. Biol.* **10**, 1255–1266
 53. Kerry, J. A., Rohde, M., and Kwok, F. (1986) *Eur. J. Biochem.* **158**, 581–585
 54. Coburn, S. P., Mahuren, J. D., Schaltenbrand, W. E., and Ericson, K. L. (2001) *FASEB J.* **15**, A963
 55. Tang, L., Li, M. H., Cao, P., Wang, F., Chang, W. R., Bach, S., Reinhardt, J., Ferandin, Y., Galons, H., Wan, Y., Gray, N., Meijer, L., Jiang, T., and Liang, D. C. (2005) *J. Biol. Chem.* **280**, 31220–31229
 56. Ortega, S., Prieto, I., Odajima, J., Martin, A., Dubus, P., Sotillo, R., Barbero, J. L., Malumbres, M., and Barbacid, M. (2003) *Nat. Genet.* **35**, 25–31
 57. Li, M. H., Kwok, F., Chang, W. R., Lau, C. K., Zhang, J. P., Lo, S. C., Jiang, T., and Liang, D. C. (2002) *J. Biol. Chem.* **277**, 46385–46390
 58. Li, M. H., Kwok, F., Chang, W. R., Liu, S. Q., Lo, S. C., Zhang, J. P., Jiang, T., and Liang, D. C. (2004) *J. Biol. Chem.* **279**, 17459–17465
 59. Percudani, R., and Peracchi, A. (2003) *EMBO Rep.* **4**, 850–854
 60. Eliot, A. C., and Kirsch, J. F. (2004) *Annu. Rev. Biochem.* **73**, 383–415
 61. Gachon, F., Fonjallaz, P., Damiola, F., Gos, P., Kodama, T., Zakany, J., Duboule, D., Petit, B., Tafti, M., and Schibler, U. (2004) *Genes Dev.* **18**, 1397–1412
 62. Mills, P. B., Surtees, R. A., Champion, M. P., Beesley, C. E., Dalton, N., Scambler, P. J., Heales, S. J. R., Briddon, A., Scheimberg, I., Hoffmann, G. F., Zschocke, J., and Clayton, P. T. (2005) *Hum. Mol. Gen.* **14**, 1077–1086